

# Fluorescence probe partitioning between $L_o/L_d$ phases in lipid membranes

Tobias Baumgart<sup>a</sup>, Geoff Hunt<sup>b</sup>, Elaine R. Farkas<sup>a</sup>, Watt W. Webb<sup>a,\*</sup>, Gerald W. Feigenson<sup>b</sup>

<sup>a</sup> School of Applied and Engineering Physics, Cornell University, Ithaca, NY 14853, USA

<sup>b</sup> Department of Molecular Biology and Genetics, Cornell University, Ithaca, NY 14853, USA

Received 11 December 2006; received in revised form 3 May 2007; accepted 11 May 2007

Available online 21 May 2007

## Abstract

Fluorescence microscopy imaging is an important technique for studying lipid membranes and is increasingly being used for examining lipid bilayer membranes, especially those showing macroscopic coexisting domains. Lipid phase coexistence is a phenomenon of potential biological significance. The identification of lipid membrane heterogeneity by fluorescence microscopy relies on membrane markers with well-defined partitioning behavior. While the partitioning of fluorophores between gel and liquid-disordered phases has been extensively characterized, the same is not true for coexisting liquid phases. We have used fluorescence microscopy imaging to examine a large variety of lipid membrane markers for their liquid phase partitioning in membranes with various lipid compositions. Most fluorescent lipid analogs are found to partition strongly into the liquid-disordered ( $L_d$ ) phase. In contrast, some fluorescent polycyclic aromatic hydrocarbons with a flat ring system were found to partition equally, but others partition preferentially into liquid-ordered ( $L_o$ ) phases. We have found these fluorescent markers effective for identification of coexisting macroscopic membrane phases in ternary lipid systems composed of phospholipids and cholesterol.

© 2007 Elsevier B.V. All rights reserved.

**Keywords:** Liquid ordered; Liquid disordered; Fluorescence microscopy; Probe partitioning; Liposome; Vesicle

## 1. Introduction

The “raft hypothesis,” which proposes that biological membranes laterally segregate into biologically relevant entities based on lipid phase separations, is currently a matter of considerable controversy and has been the focus of numerous reviews [1–13]. Despite enormous efforts to understand lateral membrane heterogeneities, the membrane phase behavior of live cells, and even simple model membrane mixtures, is currently far from being understood. For example, complex experiments that cause drastic reorganization of biological membranes, e.g. detergent resistance or major changes in cholesterol concentration, have been used to infer molecular-level details of membrane structure, leaving considerable uncertainty regarding the partitioning of membrane associated components. A variety of fluorescence approaches have been used to examine the existence and nature of lipid heterogeneities in relatively unperturbed biological membranes, including imaging of plasma

membrane lipid heterogeneities [14,15], fluorescence polarization studies [16], fluorescence red shift imaging [17], fluorescence resonance energy transfer imaging [18], and single particle tracking [19]. For the fluorescent probes used in these and other studies, the partition coefficients of fluorophores between liquid-ordered ( $L_o$ , the putative “raft” phase) and liquid-disordered ( $L_d$  or  $L_o$ ) phases are unknown. Lipid model membranes provide a means to examine the partitioning behavior of membrane fluorophores between membrane phases, for defined and equilibrated membrane compositions. The partitioning of fluorescence probes between membrane phases has been examined by a variety of techniques [20,21], and a wide range of fluorescent probes has been employed to study membrane heterogeneity [20,22].

Optically resolvable liquid-disordered/liquid-ordered phase domains in lipid model membranes have been studied by fluorescence microscopy in lipid bilayer membranes from mixtures involving at least three components [23–28]. These studies were preceded by fluorescence microscopy studies of gel/ $L_d$  phase coexistence in lipid bilayers [29–32].

Most studies to date have examined the partitioning of fluorophores between gel and  $L_d$  phase [33–39]. An important

\* Corresponding author. 212 Clark Hall, Cornell University, Ithaca, NY, 14853-2501, USA. Tel.: +1 607 255 3331; fax: +1 607 255 7658.

E-mail address: [www2@cornell.edu](mailto:www2@cornell.edu) (W.W. Webb).

finding from this body of research is that gel partitioning is increased for fluorophores with saturated chains that approximately match the thickness of one leaflet of the gel host membrane [33,35]. Probe moieties linked to alkyl chains at the chain end versus positions closer to the headgroup of amphiphilic membrane components showed larger preference for gel phases [34,36], probably due to decreased perturbation of the packing of the gel. Fluorescent lipid probes with unsaturated chains are found to partition into the disordered liquid phase [38].

Due to the need to interpret studies from fluorescence microscopy and to elucidate the biological relevance of phase coexistence, the partitioning of fluorophores between  $L_o/L_d$  phases is increasingly being addressed [40–44]. Importantly, short chain sphingolipid probes were found to have relatively low partitioning into membrane phases with putative raft-like compositions [40]. Furthermore, increased partitioning into the  $L_d$  phase versus the  $L_o$  phase was found for increasing degree of unsaturation and decreasing chain lengths, as in the case of bimane-labeled diacyl phospholipid probes [41], similar to the findings for gel/ $L_d$  coexistence mentioned above. Corresponding findings were reported in [38].

The present study examines the partitioning of fluorophores, many of which might be used for imaging lipid bilayer membranes with fluorescence microscopy techniques. To facilitate systematic comparisons, a large number of fluorophores are examined by a fixed protocol.

We first discuss the partitioning of lipid fluorophores between coexisting  $L_o$  and  $L_d$  phases for two different ternary lipid mixtures. These labeled lipids have a fluorophore either at the head group or attached to the hydrocarbon chain, or are fluorescent cholesterol derivatives or analogs. Fluorophore partitioning is determined by qualitatively comparing fluorescence intensities in coexisting domains. We discuss experimental limitations in deducing fluorophore partitioning from fluorescence microscopy imaging. We then elucidate the partitioning of several fluorescent polycyclic aromatic hydrocarbons (PAHs), because the PAH perylene was recently found to allow imaging of liquid-ordered domains coexisting with  $L_d$  domains [28]. Our findings indicate that PAHs, in contrast to the majority of fluorescent membrane markers, show a weak to pronounced affinity for  $L_o$  versus  $L_d$  phases. Finally, we determine the orientational ordering of PAHs in differing membrane phases by polarized fluorescence microscopy.

## 2. Materials and methods

### 2.1. Phospholipids and cholesterol

Brain sphingomyelin (SPM), dioleoylphosphatidylcholine (DOPC), dioleoylphosphatidylglycerol (DOPG), distearoylphosphatidylcholine (DSPC) and N-caproylamine dipalmitoylphosphatidylethanolamine were purchased from Avanti Polar Lipids, Inc. (Alabaster, AL) and used without purification after phospholipid purity was confirmed by thin-layer chromatography. Phospholipid stock solutions were quantitated by means of a phosphate assay [31]. Cholesterol (chol) was obtained from Nu Chek Prep (Elysian, MN) or Avanti Polar Lipids, and a stock solution was prepared in chloroform by standard quantitative techniques.

### 2.2. Fluorescent probes

The fluorescent probes N-(Lissamine Rhodamine B sulfonyl) dioleoyl phosphatidylethanolamine (Liss-Rho-DOPE), 1,2-dipalmitoyl-*sn*-glycero-3-phosphoethanolamine-N-(Lissamine Rhodamine B Sulfonyl) (Liss-Rho-DPPE), N-(7-nitro-2-1,3-benzoxadiazol-4-yl) dipalmitoyl phosphatidylethanolamine (NBD-DPPE), 1,2-dipalmitoyl-*sn*-glycero-3-phosphoethanolamine-N-(1-Texas Red hexanoyl), and 1,2-dioleoyl-*sn*-glycero-3-phosphoethanolamine (7-nitro-2-1,3-benzoxadiazol-4-yl) (NBD-DOPE), were purchased from Avanti Polar Lipids, Inc (Alabaster, AL).

The fluorescent probes N-(4,4-difluoro-5,7-dimethyl-4-bora-3a,4a-diaza-s-indacene-3-dodecanoyl)sphingosyl phosphocholine (Bodipy- $C_{12}$ -SPM), N-(4,4-difluoro-5,7-dimethyl-4-bora-3a,4a-diaza-s-indacene-3-pentanoyl)sphingosyl phosphocholine (Bodipy- $C_5$ -SPM), 2-(4,4-difluoro-5,7-dimethyl-4-bora-3a,4a-diaza-s-indacene-3-pentanoyl)-1-hexadecanoyl-*sn*-glycero-2-phosphocholine (Bodipy-PC), 3,3'-dilinoleoyloxycarbocyanine perchlorate (DiO- $C_{18}:2$ ), 1,1'-didodecyl-3,3,3',3'-tetramethylindocarbocyanine perchlorate (DiI- $C_{12}:0$ ), 1,1'-dihexadecyl-3,3,3',3'-tetramethylindocarbocyanine perchlorate (DiI- $C_{16}:0$ ), 1,1'-dioctadecyl-3,3,3',3'-tetramethylindocarbocyanine perchlorate (DiI- $C_{18}:0$ ), 1,1'-dieicosanyl-3,3,3',3'-tetramethylindocarbocyanine perchlorate (DiI- $C_{20}:0$ ), 1,1'-didocosanyl-3,3,3',3'-tetramethylindocarbocyanine perchlorate (DiI- $C_{22}:0$ ), 1,1'-dioleoyl-3,3,3',3'-tetramethylindocarbocyanine perchlorate (DiI- $C_{18}:1$ ), 3,6-bis(diethylamino)-9-(2-octadecyloxy) carbonylphenyl, chloride (R18), and 22-(N-(7-nitrobenz-2-oxa-1,3-diazol-4-yl)amino)-23,24-bisnor-5-cholesterol-3-ol (NBD-chol) were purchased from Molecular Probes (Eugene, OR).

The fluorophore Texas-red N-caproylamine DPPE was synthesized from N-caproyl dipalmitoylphosphatidylethanolamine according to a procedure described in [45]. Cholestatrienol was synthesized according to Fischer et al. [46].

Naphtho[2,3a]-pyrene, perylene, and rubicene, and *N,N*,bis-dimethylphenyl 2,4,6,8, perylenetetracarboxyl diamide (PERY) were purchased from Sigma-Aldrich Corp. (St. Louis, MO). Terrylene was obtained from Chiron AS Chemicals (Trondheim, Norway).

### 2.3. Preparing GUVs

Giant unilamellar vesicles (GUVs) were prepared according to the procedure described by Akashi et al. [47], with a few variations. Alternatively, the method of electrosweeling was employed [48]. Both methods led to identical phase behavior and equivalent probe partitioning, determined by fluorescence microscopy, excluding electrode effects [49] to contribute to our findings. In both cases, GUVs were formed at a temperature of 65 °C, which ensured vesicle formation from homogenous bilayer membranes. In the case of the Akashi method, the buffer was 2 mM Pipes, 10 mM KCl, and 1 mM EDTA, pH=7.0. Stock solutions of DOPC in chloroform contained 10 mol% DOPG, since charged phospholipids are necessary for preparing GUVs by this method [47]. Stock solutions of SPM and DSPC in chloroform contained no additional charged lipids. With the electrosweeling method, stock solutions did not contain charged lipids. For this method, GUVs were swelled using an alternating electric field applied for 2 h in a sucrose solution (100 mM) [48]. Following either preparation method, GUVs were slowly cooled (~1–2 °C/h) to room temperature (~23 °C), deposited onto #1 coverslips, and enclosed by a clean glass slide containing a ring of silicone high-vacuum grease as a surrounding seal and spacer.

Ternary lipid mixtures used to prepare GUVs were SPM/DOPC/chol and DSPC/DOPC/chol. The vesicle composition for vesicles with liquid phase coexistence was 27/50/23 (molar ratios of SPM or DSPC/DOPC/chol), except for the vesicle shown in Fig. 3e and f, which had a composition of SPM/DOPC/chol=30/45/25. Most fluorescent probes were added at a concentration of 0.1 mol%. The fluorescent probes Bodipy- $C_{12}$ -SPM, Bodipy- $C_5$ -SPM, and NBD-chol were added at concentrations of 0.2 mol%. The fluorescent probes perylene, naphthopyrene, rubicene and terrylene were added at concentrations of 0.5 mol%.

### 2.4. Microscopy

GUVs were imaged with either confocal microscopy using a Leica TCS SP2 spectral confocal system (Leica Microsystems Inc, Bannockburn, IL) or by two-

photon excitation microscopy using a homebuilt multiphoton laser scanning microscope (W.R. Zipfel, Cornell University) based on a Bio-Rad 1024 scanhead (Bio-Rad, Richmond, CA), using a two-photon excitation wavelength of  $\lambda = 750$  nm. In case of confocal one-photon excitation microscopy, the following wavelengths were used for excitation: 458 nm (naphthopyrene), 488 nm (Bodipy, DiO, NBD, rubicene, PERY), and 568 nm (DiI, Lissamine rhodamine, Texas red, R18). Cholestatrienol was imaged by wide-field illumination using a bandpass excitation filter centered at 340 nm (width 30 nm). For all probes examined, partitioning was determined for vesicles labeled with one dye only to avoid bleed-through into different detector channels. Membrane phase assignment was checked by double labeling vesicles with the probe of interest and another probe of known partitioning behavior. Angular emission patterns were determined by imaging equatorial sections of homogenous vesicles using linearly polarized light, and extracting the angular intensity profiles from the obtained fluorescence micrographs by means of a tracing algorithm. Each angular profile consisted of averaged measurements of ten different vesicles. All images were obtained at room temperature.

### 3. Results

A total of 26 lipid membrane probes (see Figs. 1 and 2 for molecular structures) were used to examine the principles that govern the partitioning of membrane fluorophores between coexisting liquid membrane phases in giant unilamellar vesicles. In order to identify molecular factors governing probe partitioning, we examined dye distributions between two coexisting liquid phases, a liquid ordered ( $L_o$ ) and a liquid disordered ( $L_d$ ) phase, in vesicles made of ternary lipid mixtures with identical compositions. In order to determine potential differences in probe partitioning in vesicles with the same lipid ratios but different ordered phase-preferring lipid type, we compared fluorophore partitioning in two different lipid systems. The ternary lipid mixtures used were SPM/DOPC/cholesterol and DSPC/DOPC/cholesterol. All vesicles (except where indicated) had a composition of 27/50/23 (molar ratios of SPM or DSPC/DOPC/cholesterol).

Phase assignment of GUVs imaged by fluorescence microscopy was accomplished by determining the following membrane phase features: (a) area fraction, (b) continuity (connectivity), and (c) partitioning of fluorophores with known partitioning behavior. According to published phase diagrams of ternary lipid mixtures [26,32], the composition of our vesicles leads to segregation into a DOPC rich majority  $L_d$  phase, and a DSPC- or SPM-rich  $L_o$  minority phase. Phase assignment was verified using the fluorophore Liss-Rho-DOPE, which had previously been found to partition strongly out of  $L_o$  phases coexisting with  $L_d$  phases [23].

Figs. 1 and 2 show the molecular structures of all the fluorophores that were examined. The dyes may be categorized as follows: (a) phospholipids with unsaturated acyl chains and a headgroup label (NBD-DOPE and Liss-Rho-DOPE); (b) phospholipids with saturated acyl chains and a headgroup label (NBD-DPPE, Texas-Red-DPPE and Liss-Rho-DPPE); (c) phospholipids with saturated acyl chains and a label attached to the headgroup via a caproyl spacer (Texas-red-N-caproylamine-DPPE); (d) carbocyanine dyes with saturated hydrocarbon chains (DiI  $C_n:0$  with  $n = 12, 16, 18, 20, 22$ ); (e) carbocyanine dyes with unsaturated lipid chains (DiO C18:2 (fast) and DiI C18:1); (f) chain-labeled phospholipids (Bodipy-C5-PC, Bodipy-

C5-SPM, and Bodipy-C12-SPM, Bodipy-ceramide); (g) single alkyl chain membrane probes (R18); (h) a labeled cholesterol analog (NBD-chole); (i) the fluorescent cholesterol analog cholestatrienol; (j) fluorescent polycyclic aromatic hydrocarbons (naphthopyrene, rubicene, perylene, terrylene, and “PERY”); (k) the fluorescent hydrophobic membrane marker DPH.

Tables 1 and 2 summarize the partitioning behavior of all the fluorescent membrane probes used in this study. In these tables, the partitioning of fluorophores is divided into three categories distinguishing  $L_o$  phase or  $L_d$  phase preference, and equal partitioning into either  $L_o$  or  $L_d$  phases. In principle, fluorescence microscopy allows the quantitation of fluorophore partitioning (in terms of *partition coefficients*). Such a quantitative approach is challenging beyond the usual problems of background subtraction and shading corrections over the image, requiring careful correction for effects such as concentration-dependent self-quenching, the influence of each membrane phase on fluorescence intensity due to fluorophore environmental sensitivity, and selective excitation due to confined fluorophore orientations in differing phases (see below). Therefore, we report here the qualitative partitioning behavior of these 26 probes.

Table 1 summarizes the observed partitioning behavior of all fluorophores in the SPM system. Qualitatively similar partitioning behavior was found in the DSPC system, with the important exception of saturated chain DiI dyes (see below). The behavior of these dyes is depicted in Table 2.

In every case, fluorescent membrane markers that contained unsaturated alkyl chains or fluorophore-labeled chains as membrane anchors were observed by confocal fluorescence microscopy to partition strongly out of the  $L_o$  phase, and into the  $L_d$  phase. This overarching observation applies to both the DSPC and the SPM ternary lipid systems. A representative example is shown in Fig. 3a, which displays a hemispherical projection of a vesicle (DSPC system) labeled with the fluorophore Liss-Rho-DOPE. In this vesicle, a brightly labeled  $L_d$  domain is found (in Fig. 3a and all following images of phase separated vesicles, a white arrow points to the  $L_d$  phase), whereas in the  $L_o$  phase matrix, hardly any fluorescence could be detected. Liquid-disordered phases of the mixtures used in the present study are enriched in DOPC relative to the coexisting liquid-ordered phases. Strong partitioning into the  $L_d$  phase (coexisting with an  $L_o$  phase) of probes with unsaturated alkyl chains is therefore expected and has been observed in previous microscopy studies [23].

Lipids labeled in the chain region with the Bodipy fluorophore partitioned preferentially into the  $L_d$  phase for both mixtures examined in this study. The membrane dye Bodipy-PC had previously been observed to partition preferentially into  $L_d$  phases coexisting with gel phase domains [30]. Fig. 3b shows a vesicle of the DSPC system in which Bodipy-PC shows fluorescence in  $L_d$  phase domains rather than in the coexisting  $L_o$  phase domains. Note that inhomogeneous fluorescence intensity levels within homogenous membrane phases in Figs. 3 and 4 result from vesicle movement during imaging, membrane assemblies near the imaged vesicle, and collection of sub-

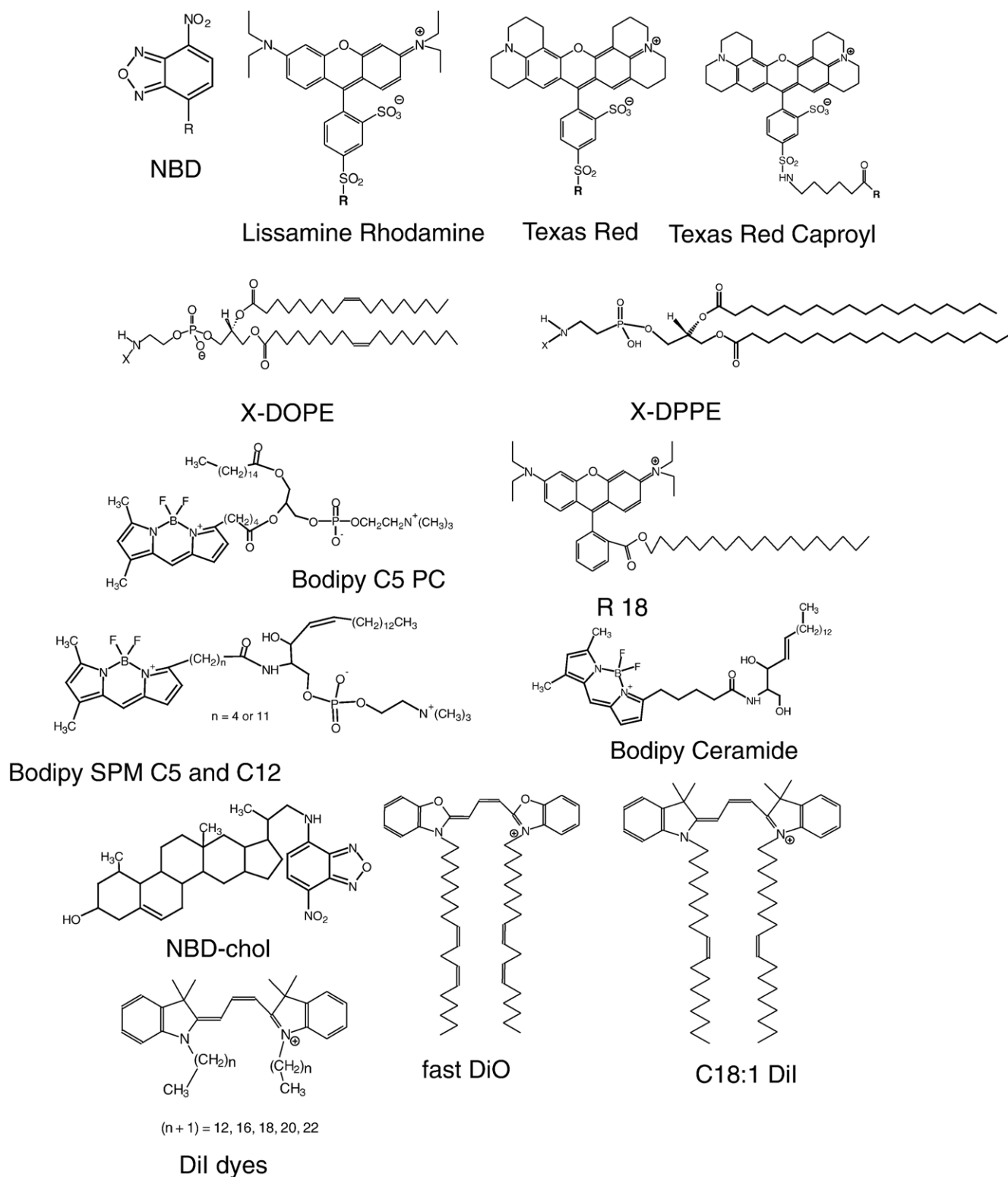


Fig. 1. Lipid analog dyes used for partitioning studies: mostly disordered phase preferring probes (see the text for the exception of long chain DiI probes in the DSPC system).

optimal numbers of confocal slices for hemispherical projections. The sphingomyelin-derived fluorophore Bodipy-C5-SPM has been interpreted in the past to mimic the properties of endogenous sphingomyelin in biological cell membranes, particularly to study intracellular membrane trafficking path-

ways [50–52]. The partitioning of Bodipy-C5-SPM, Bodipy-C12-SPM and Bodipy-Ceramide were therefore examined in vesicles containing sphingomyelin-enriched  $L_o$  domains. All three dyes are observed to partition strongly out of the sphingomyelin-rich  $L_o$  phase matrix and into  $L_d$  phase domains



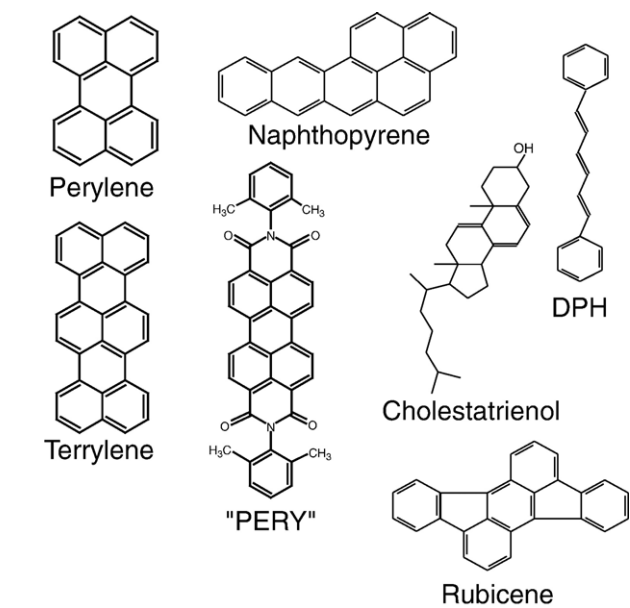


Fig. 2. PAH dyes and DPH used for partitioning and probe orientation studies. The molecules perylene, naphthopyrene, terrylene, cholestatrienol and rubicene partition equally or preferentially into the *L*<sub>o</sub> phase. The dye PERY is *L*<sub>d</sub> phase preferring and DPH does not show preferential partitioning.

(images not shown), both in the DSPC and in the SPM system. This finding is in accordance with results from Wang and Silvius, who determined probe partitioning by an inter-vesicle partitioning method [40]. They found Bodipy-C5-SPM to partition preferentially out of sphingomyelin-enriched *L*<sub>o</sub> domains. As these authors noted, caution is needed when relating studies of membrane trafficking with short chain

Table 1  
Partitioning of fluorescent lipid mimetic molecules between two coexisting fluid membrane phases in the ternary lipid mixture SPM/DOPC/cholesterol

Fluorescent probe	Partitioning preference (= indicates no preference)
X-DOPE	<i>L</i> <sub>d</sub>
DiI C18:1	<i>L</i> <sub>d</sub>
Fast DiO	<i>L</i> <sub>d</sub>
Bodipy PC	<i>L</i> <sub>d</sub>
SPM C <sub>n</sub> Bodipy	<i>L</i> <sub>d</sub>
Bodipy Ceramide	<i>L</i> <sub>d</sub>
X-DPPE	<i>L</i> <sub>d</sub>
Y-DPPE	<i>L</i> <sub>d</sub>
R18	<i>L</i> <sub>d</sub>
NBD-cho1	<i>L</i> <sub>d</sub>
Cholestatrienol	<i>L</i> <sub>o</sub>
DiI C <sub>m</sub> :0	<i>L</i> <sub>d</sub>
Naphthopyrene	<i>L</i> <sub>o</sub>
Perylene	=
Rubicene	=
Terrylene	<i>L</i> <sub>o</sub>
DPH	=
"PERY"	<i>L</i> <sub>d</sub>

The partitioning behavior of the fluorophores indicated in this table for the SPM system is qualitatively similar in the DSPC system. The saturated chain DiI dyes are the important exception (see Table 2). X=NBD, Lissamine rhodamine. Y=Texas red, N-caproyl-Texas red. *n*=5, 12. *m*=12, 16, 18, 20, 22.

Table 2  
Comparison of the partitioning of saturated chain dialkylindocarbocyanine dyes of varying chain lengths in ternary lipid mixtures with liquid phase coexistence

Fluorescent probe	Phase preference SPM system	Phase preference DSPC system
DiI C12:0	<i>L</i> <sub>d</sub>	<i>L</i> <sub>d</sub>
DiI C16:0	<i>L</i> <sub>d</sub>	<i>L</i> <sub>d</sub>
DiI C18:0	<i>L</i> <sub>d</sub>	<i>L</i> <sub>o</sub>
DiI C20:0	<i>L</i> <sub>d</sub>	<i>L</i> <sub>o</sub>
DiI C22:0	<i>L</i> <sub>d</sub>	<i>L</i> <sub>o</sub>

fluorescent sphingomyelin probes to heterogeneous membrane distributions of endogenous sphingomyelins [40].

Since *L*<sub>o</sub> phases are enriched in long-chain saturated lipids, the present study examined the partitioning behavior of long and saturated chain, head group labeled membrane dyes derived from DPPE. Dietrich et al., using planar supported membranes of the SPM/POPC/chol system [24] (composition 0.25/0.5/

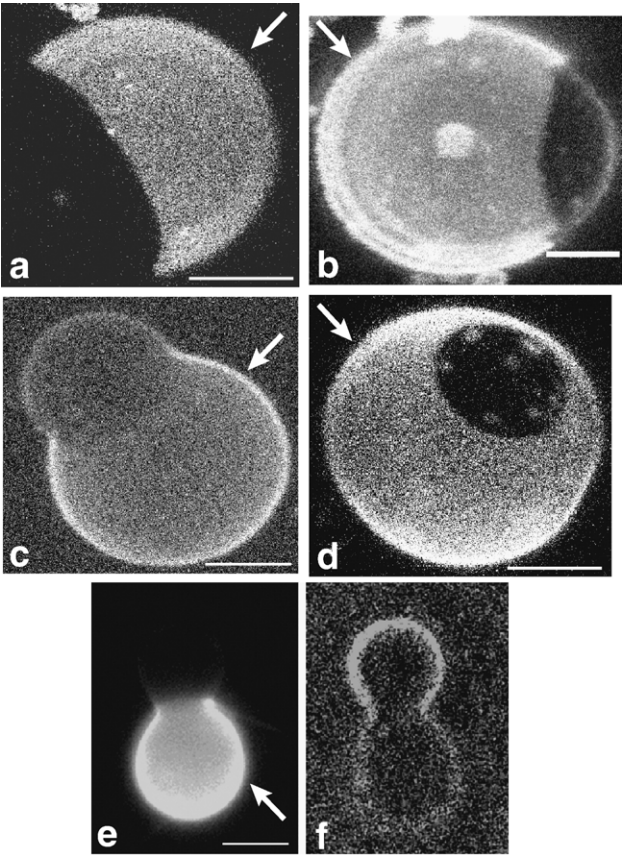


Fig. 3. Hemispherical projections of confocal images of GUVs, labeled with a variety of different membrane dyes. In all panels of this figure, and all following figures, the *L*<sub>d</sub> phase is indicated with a white arrow. Panels a–d refer to composition 27/50/23 (DSPC/DOPC/chol), where the *L*<sub>d</sub> phase is the majority phase. (a) Liss-Rho-DOPE: *L*<sub>d</sub> phase partitioning preference is found for this dye as well as other dyes with unsaturated chains. (b) Bodipy-PC: Lipids labeled in the chain region partition into the *L*<sub>d</sub> phase. (c and d) NBD-DPPE and Liss-Rho-DPPE, respectively: long and saturated chain headgroup labeled lipids prefer the *L*<sub>d</sub> phase. (e and f) Rho-DOPE (e) and cholestatrienol (f) labeling of a vesicle in the SPM system with composition 30/45/25 (SPM/DOPC/chol). Cholestatrienol is observed to preferentially partition into the *L*<sub>o</sub> phase, whereas Rho-DOPE labels the *L*<sub>d</sub> phase. Bars: 5 μm (a–d) and 15 μm (e–f).

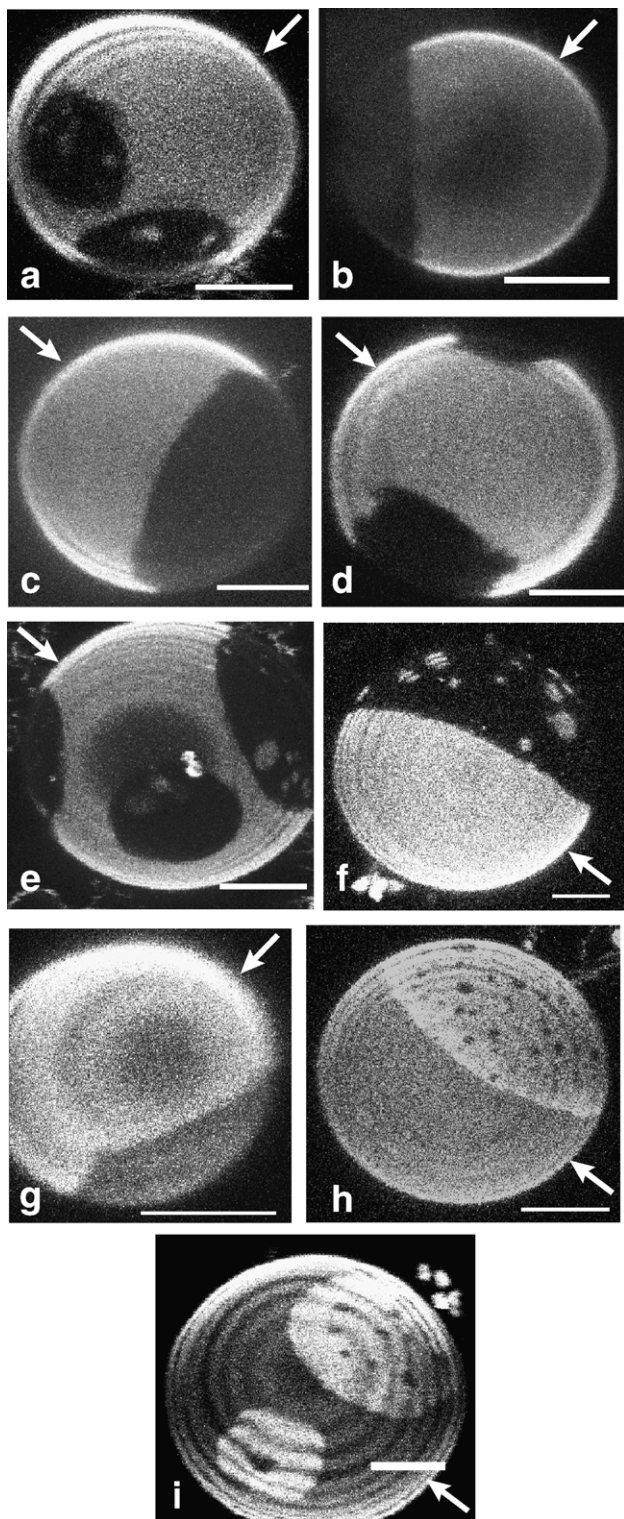


Fig. 4. Confocal images of GUVs in the SPM/DOPC/chol system (a–e) and the DSPC/DOPC/chol system (f–i). In all images the  $L_d$  phase is the majority phase (i.e. the phase with larger area fraction). The following DiI fluorophores were used for labeling: (a and f), DiI-C12:0; (b and g), DiI-C16:0; (c and h), DiI-C18:0; (d) DiI C20:0; and (e and i), DiI C22:0. In the SPM system, DiI dyes of all chain lengths partitioned into the  $L_d$  phase as in panels a–e. In the DSPC system, however, long saturated chain DiIs partitioned preferentially into the  $L_o$  phase as in panels h–i. Note that the concentric shading in several images is due to z scan inhomogeneity, not membrane inhomogeneity. Bar: 5  $\mu$ m.

0.25), observed that the fluorophore NBD-DPPE partitioned with modest preference into the  $L_o$  phase, while the fluorophore Texas-red-DPPE strongly preferred the  $L_d$  phase [24]. Similar partitioning behavior of Texas-red-DPPE was also found by Veatch et al. [26] in GUVs of a range of different compositions. We found that for all DPPE-derived probes used in the present study (see Table 1), strong preference for liquid-disordered phases was observed in both SPM and DSPC systems. Fig. 3c and d show this partitioning behavior for the fluorophores NBD-DPPE and Liss-Rho-DPPE, respectively, in the DSPC system. This finding implies that the presence of a bulky fluorophore in the headgroup region disturbs lipid packing in that part of an  $L_o$  phase membrane, which leads to preferential exclusion of these fluorophores from the  $L_o$  phase if the  $L_o$  phase coexists with a disordered liquid phase. This explanation is supported by Samsonov et al., who found the fluorophore N-Bodipy-GM1 to be enriched in  $L_o$  phase domains [23]. In that case, the fluorophore was effectively separated from the headgroup region by a sugar spacer. We therefore synthesized N-caproylamine-Texas-Red-DPPE, where the fluorophore is separated from the headgroup region by a 6-carbon caproyl spacer. Again, however, strong partitioning of this dye out of  $L_o$  and into coexisting  $L_d$  phases was observed in both of the ternary systems examined. This effect is likely not due to exclusion of the ethanolamine part of the headgroup from the PC-rich  $L_o$  region, because the Silvius group found that the nature of the lipid headgroup only weakly influenced lipid partitioning between  $L_o$  and  $L_d$  phases when comparing phosphatidylcholine, sphingomyelin, glycosphingolipids, and the ganglioside GM1 [43]. Thus, despite the presence of a caproyl spacer, the partitioning of the membrane probe N-caproyl-Texas-Red-DPPE is probably dominated by the presence of a large and bulky fluorophore attached to the ethanolamine headgroup. Based on this finding, we suggest that the saccharide moieties of gangliosides must be able to pack more efficiently into the headgroup region of SPM-rich  $L_o$  phases or alternatively, more effectively prevent the bulky fluorophore from perturbing the membrane surface.

The dialkylcarbocyanine dyes, DiI, are among the most widely used fluorescent membrane probes, in part because of brightness and photostability, and in part because of their availability with a variety of hydrocarbon chains. These dyes have been employed for imaging membrane heterogeneity in cellular membranes [14,15], and some were found to enrich in ordered regions with properties similar to detergent resistant membranes [15], which have been assumed to be in the  $L_o$  phase state [53]. However, as shown in Fig. 4a to e, none of these DiI probes preferentially partitioned into sphingomyelin-rich  $L_o$  domains. DiI dyes with saturated chains of lengths 12, 16, 18, 20 and 22 carbons partitioned strongly out of  $L_o$  and into the  $L_d$  phase in the SPM system. However, in the DSPC system, DiI with chain lengths 18, 20 and 22 partitioned preferentially into the  $L_o$  phase (see Fig. 4i–j), whereas the shorter chain lengths (12 and 16 carbons) partitioned into the  $L_d$  phase (see Fig. 4g and h). The partitioning behavior of DiI dyes in both of the ternary systems is summarized in Table 2. The finding of a difference in long chain DiI dye partitioning in quasi-ternary SPM and DSPC



systems is supported by an equivalent previous result for the DiI C18 dye [54].

Indocarbocyanine fluorophores with unsaturated alkyl chains (DiI C18:1, fast DiO) partitioned strongly into the  $L_d$  phase in both the SPM and DSPC systems. The single chain amphiphilic fluorophore R18 was also observed to partition strongly out of  $L_o$  domains and into  $L_d$  domains, for both the DSPC and the SPM systems (images not shown).

Cholesterol is expected to enrich in  $L_o$  phases relative to coexisting  $L_d$  phases, according to the tie line directions in lipid systems similar to the ones examined in the present research [55]. However, the cholesterol derivative NBD-chol partitioned out of  $L_o$  domains and into  $L_d$  domains (images not shown). This finding underscores the fact that NBD-chol is a label that does not mimic the properties of unmodified cholesterol, as has been pointed out previously [56]. We found that cholestatrienol does enrich in  $L_o$  domains in the sphingomyelin system, as indicated in Fig. 3 e–f. The fluorophore, however, bleaches quickly and high quality images are difficult to obtain. It has been found that cholestatrienol, a fluorescent cholesterol derivative, mimics endogenous cholesterol even better [56] than the commercially available fluorescent dehydroergosterol that has been employed as a fluorescent cholesterol analog for microscopy studies of cellular membranes [15].

### 3.1. Partitioning of fluorescent polycyclic aromatic hydrocarbons

Several fluorescent polycyclic aromatic hydrocarbons show sufficient quantum yield, photostability and wavelength characteristics to make them suitable for fluorescence microscopy. Their partitioning behavior was therefore of great interest.

In a search for probes that allow imaging  $L_o$  phase membranes, we focused on polycyclic aromatic hydrocarbons that were not attached to lipid analogs [44]. We tested the possibility that these dyes would mimic the packing properties of cholesterol, given their flat, disk-shaped molecular structure.

The highly photostable fluorophore perylene has long been used as a fluorescent membrane dye for spectroscopic studies [57–59]. More recently, perylene has enabled two-color fluorescence microscopy of coexisting liquid phases. Perylene was found to preferentially label  $L_o$  phases in ternary lipid mixtures containing egg sphingomyelin, DOPC, and cholesterol [28]. Fig. 5a shows that perylene does not show preferential partitioning in ternary mixtures containing brain sphingomyelin, though (compare 5b which shows Liss-Rho-DOPE partitioning in the same vesicle as 5a to indicate phase coexistence). Rubicene is another polycyclic aromatic hydrocarbon with high photostability that can be used for microscopy imaging. Similar to perylene, rubicene showed partitioning that very weakly favors the  $L_o$  phase between liquid-ordered and disordered phases (data not shown). Naphthopyrene shows stronger partitioning into  $L_o$  phases in the brain sphingomyelin system (Fig. 5c, compare 5d which shows Liss-Rho-DOPE partitioning in the same vesicle). Similarly, preferential  $L_o$  phase partitioning is found with the fluorophore terrylene (Fig. 5e).

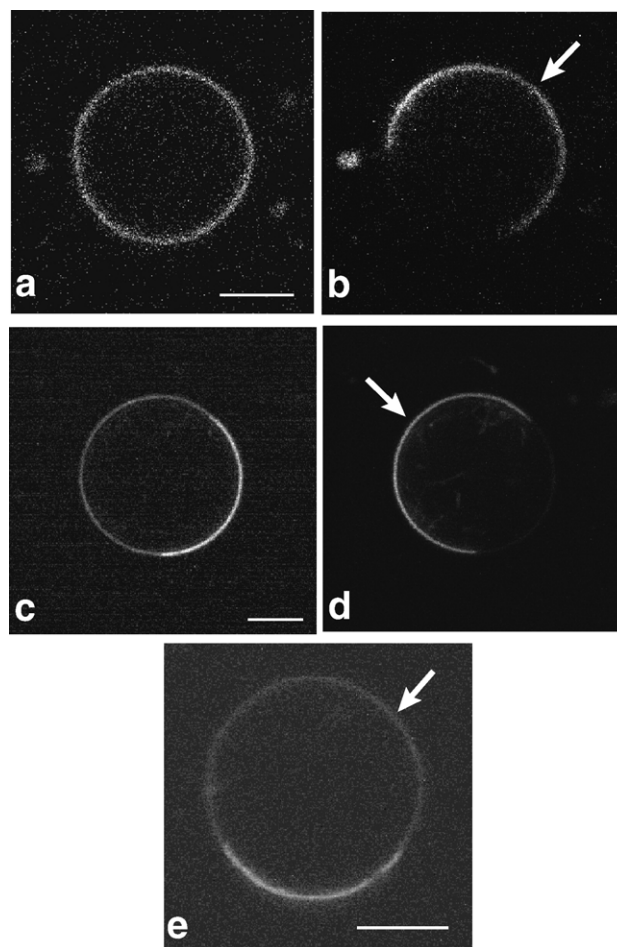


Fig. 5. Equatorial images of GUVs obtained by two-photon laser scanning microscopy at an excitation wavelength of  $\lambda = 750$  nm, indicating the partitioning of polycyclic fluorescent hydrocarbons. Images report on SPM system. (a) perylene fluorescence not distinguishing  $L_o$  and  $L_d$  phase; (b) same vesicle as in panel (a) the red fluorophore Liss-Rho-DOPE is used to image the  $L_d$  phase (c) naphthopyrene fluorescence showing phase separation; (d) same vesicle as in panel (c), Liss-Rho-DOPE fluorescence; and (e) terrylene fluorescence showing phase separation. Polycyclic aromatic hydrocarbons show equal partitioning to significant partitioning into the  $L_o$  phase, with a degree of partitioning that depends on the molecular structure of the PAH. Bar: 5  $\mu$ m.

In order to further examine the molecular features that lead fluorophores to enrich in the liquid-ordered phase, we labeled vesicles with the bi-substituted perylene derivative PERY. The bis-dimethylphenyl groups of this fluorophore are known to be able to rotate around the C–N bond [60]. This molecular feature, as well as the polar additions to the perylene backbone, differs from the flat and rigid hydrocarbon disks of the other PAHs studied. As indicated in Fig. 6a, PERY is indeed observed to partition strongly out of the ordered and into the disordered liquid phase, in both the SPM and DSPC systems. This observation supports our finding that polycyclic aromatic dyes partition into the  $L_o$  phase only in the case of hydrophobic molecules with a rigid ring system that does not obstruct lipid chain packing.

We also examined the partitioning of the membrane fluorophore DPH. Lipid-bound analogs of DPH, and DPH itself, have been used in numerous studies to analyze chain ordering in

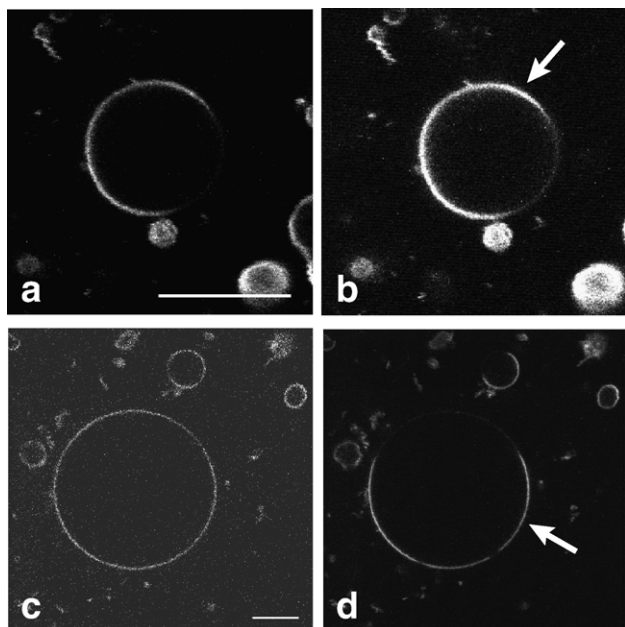


Fig. 6. Equatorial images of GUVs in the SPM system obtained by two-photon laser scanning microscopy at an excitation wavelength of  $\lambda = 750$  nm, showing the partitioning of the fluorescent membrane dyes *N,N*-bis-dimethylphenyl 2,4,6,8, perylenetetracarboxyl diamide (“PERY”) (a) and DPH (c). For comparison, the partitioning of Liss-Rho-DOPE is shown in the right image of each row (b and d), for the same vesicle imaged on the left-hand side. “PERY” strongly partitions out of  $L_o$  phases and DPH shows negligible phase preference. Bar: 12  $\mu$ m.

lipid model membranes [61,62] as well as cellular membranes [16]. The partition coefficients between cholesterol- and DPPC-rich liquid-ordered phases and pure DPPC above the main phase transition temperature (liquid-disordered phase) have been described as being close to unity [16,63]. Fig. 6c indicates that in the ternary lipid mixture SPM/DOPC/cholesterol, DPH shows a negligible partitioning difference for the mixing ratio examined in the present study. Similar partitioning was found in the DSPC system. While DPH is a nonpolar fluorophore, it lacks the rigid ring structure that leads to preferred liquid-ordered phase partitioning.

### 3.2. Orientation of hydrophobic membrane markers in $L_o$ and $L_d$ phases

In order to elucidate why disk-shaped hydrophobic polycyclic hydrocarbons partition preferentially into liquid-ordered phases, we qualitatively determined probe orientations with respect to the membrane normal direction by using polarized excitation fluorescence microscopy. To this end, optically homogenous vesicles of either  $L_d$  phase or  $L_o$  phase state were illuminated with linearly polarized light and imaged in the equatorial planes. Fig. 7 compares the intensity patterns of Liss-Rho-DOPE (second image in each panel) versus perylene, naphthopyrene and terylene, respectively, in  $L_d$  phase vesicles (pure DOPC, left column) and  $L_o$  phase vesicles (SPM/chol=1/1, right column). The excitation light polarization direction used for all images shown in Fig. 7 is indicated by the white arrow in Fig. 7a.

For all three PAHs and for Liss-Rho-DOPE, the directions of absorption and emission dipole moments point roughly along the longest axis of the dye molecule. The angular emission patterns of GUVs obtained with linearly polarized excitation can therefore be used to infer average membrane probe orientations [64–66]. A (headgroup-labeled) Liss-Rho lipid analog was previously found to orient, on average, parallel to the membrane, i.e. transition dipole moments of the fluorophore are tangent to the plane of the membrane [66]. Given the excitation light polarization direction (see arrow in Fig. 7), this fluorophore is observed to emit at higher intensities towards left and right parts of the vesicles, as expected. This behavior is shown in Fig. 7.

All three PAHs showed approximately uniform angular emission patterns for  $L_d$  phase vesicles (consisting of DOPC membranes). This finding seems to indicate random orientations of excitation dipole moments of these PAHs in  $L_d$  phase membranes. In contrast to this finding, for  $L_o$  phase vesicles, we observed for all three PAHs an angular emission pattern that was rotated by  $90^\circ$  compared to the Liss-Rho-DOPE pattern. This indicates that in the  $L_o$  phase, PAH excitation dipole moments are oriented preferentially along the membrane normal. This observation is in accordance with PAHs intercalating into liquid-ordered membranes in a way similar to cholesterol, i.e. by association of the flat surface of a disk shaped molecule with the saturated lipid chains in the  $L_o$  phase.

Fig. 8 depicts angular normalized fluorescence intensity traces, obtained from microscopy images equivalent to those shown in Fig. 7. The relative intensity differences comparing intensity maxima and minima of angular emission patterns (Fig. 8) are related to the width of a probe’s orientational probability distribution [65,67]. Larger PAHs like terylene might experience a stronger confinement in lipid membranes compared to smaller PAHs like perylene. Fig. 8a–e indicates that perylene shows a shallower angular emission intensity profile in  $L_o$  phase GUVs consisting of SPM/chol=1/1 compared to naphthopyrene and terylene in vesicles with the same lipid mixtures. This finding parallels the partitioning tendency of the fluorophores between coexisting  $L_d$  and  $L_o$  phases described above. Increased orientational confinement compared to pure DOPC membranes is also observed in DOPC membranes containing 30 mol% of cholesterol, as Fig. 8e–f show. The ordering effect of cholesterol is weaker in DOPC/chol compared to SPM/chol membranes (Fig. 8f). Liquid-ordered-like nature of cholesterol containing DOPC membranes has recently been found by NMR spectroscopy [68].

## 4. Discussion

The present study examined the partitioning behavior of fluorophores suitable for fluorescence microscopy imaging, between coexisting liquid-ordered and disordered phases. An important conclusion is that caution is necessary when choosing fluorescent membrane markers to label specific environments in either model membranes or biological membranes.

In particular, we found that a large variety of headgroup and chain-labeled fluorophores partition out of the  $L_o$  and into the



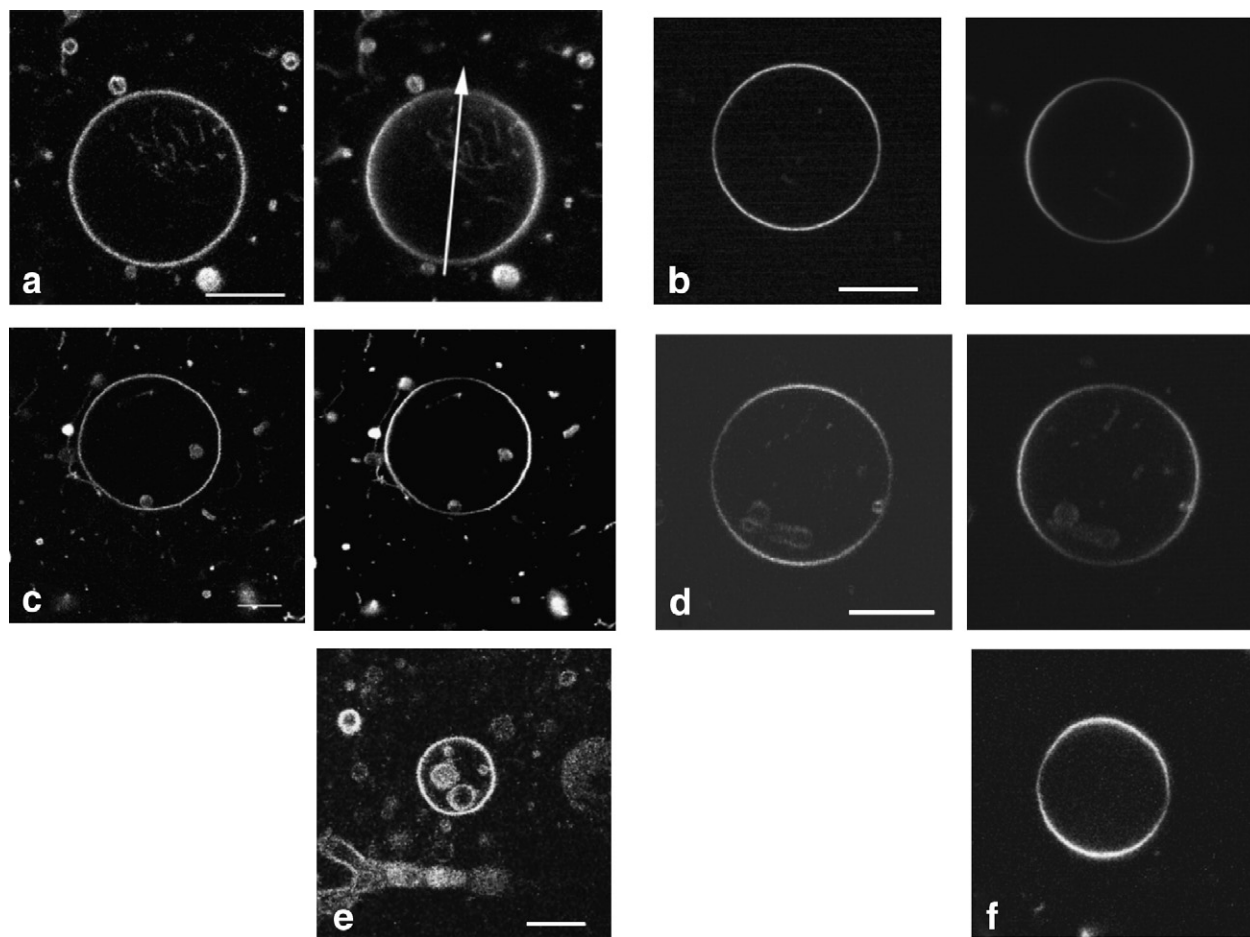


Fig. 7. Equatorial images of GUVs obtained by two-photon laser scanning microscopy at an excitation wavelength of  $\lambda = 750$  nm. Vesicles were illuminated with linear polarization along the arrow in panel a. The observed angular intensity patterns demonstrate the orientation (see text for details) of polycyclic aromatic hydrocarbons in  $L_d$  phase vesicles (DOPC) and  $L_o$  phase vesicles (SPM/chol=1:1). (a) perylene  $L_d$ ; (b) perylene  $L_o$ ; (c) naphthopyrene  $L_d$ ; (d) naphthopyrene  $L_o$ ; (e) terrylene  $L_d$ ; and (f) terrylene  $L_o$ . In case of images (a–d), the right image in each panel shows the angular fluorescence pattern of Liss-Rho-DOPE in the same vesicle, for comparison. Whereas PAH fluorescence intensities are constant around the vesicle perimeter in case of  $L_d$  phase membranes,  $L_o$  phase membranes PAHs show an angular intensity pattern that is rotated by  $90^\circ$  compared to the intensity pattern of Liss-Rho-DOPE fluorescence. This finding indicates that PAHs tend to orient with their long axes parallel to the membrane normal in  $L_o$  phase membranes, but not in  $L_d$  phase membranes. Bar: 12  $\mu$ m.

$L_d$  phase. The partitioning of DPPE and SPM-derived probes, as well as NBD-chol indicates that the phase preference of these fluorophores is dominated by the fluorescent label and not by the lipid backbone.

The partitioning of fluorophores depends on the lipid host system. The saturated-chain DiI derivatives partition increasingly into DSPC-containing  $L_o$  phases the longer the probe chain length. However, in the SPM system all DiI dyes were strongly excluded from the  $L_o$  phase. This finding shows that sphingomyelin-based  $L_o$  phases have significantly different properties compared to phosphatidylcholine  $L_o$  phases. A preferential interaction of cholesterol with sphingomyelin rather than phosphatidylcholine with long saturated chains has been suggested, but is discussed with great controversy [69,70]. We infer that the strong partitioning of DiI dyes in the SPM system out of  $L_o$  domains for all chain lengths indicates major headgroup packing constraints in the SPM system that are absent or reduced in the DSPC system. We note again that partitioning determined by fluorescence microscopy is qualitative in nature, due to reasons mentioned above. In fact, it was

recently demonstrated that DiI dyes show higher molecular brightness in  $L_o$  phases compared to  $L_d$  and gel phases (Zhao and Feigenson et al, unpublished data). This fact, alone, however, cannot explain the chain length influence on optically determined dye partitioning, described above.

The saturated chain DiI probes show strong partitioning differences depending on their chain lengths in the DSPC system. The chain length influence of DiI partitioning between  $L_d$  phases and coexisting gel phases has been analyzed previously in DMPC [33], and in DPPC and DSPC [35]. In DMPC membranes, dialkyl DiI dyes with chain lengths of 10 to 14 carbons partitioned into the liquid phase, while dyes with 16 and 18 carbons partitioned into the gel phase. In DSPC membranes, the chain length influence of dialkyl DiI partitioning between gel and liquid phase is more pronounced, with a clear maximum partitioning into the gel that matched the probe hydrocarbon chain length [35]. This behavior is also observed in the DSPC-enriched  $L_o$  phase domains shown in Fig. 4f–i and is probably due to approximate hydrophobic matching of dye and matrix lipid chains [33,35].

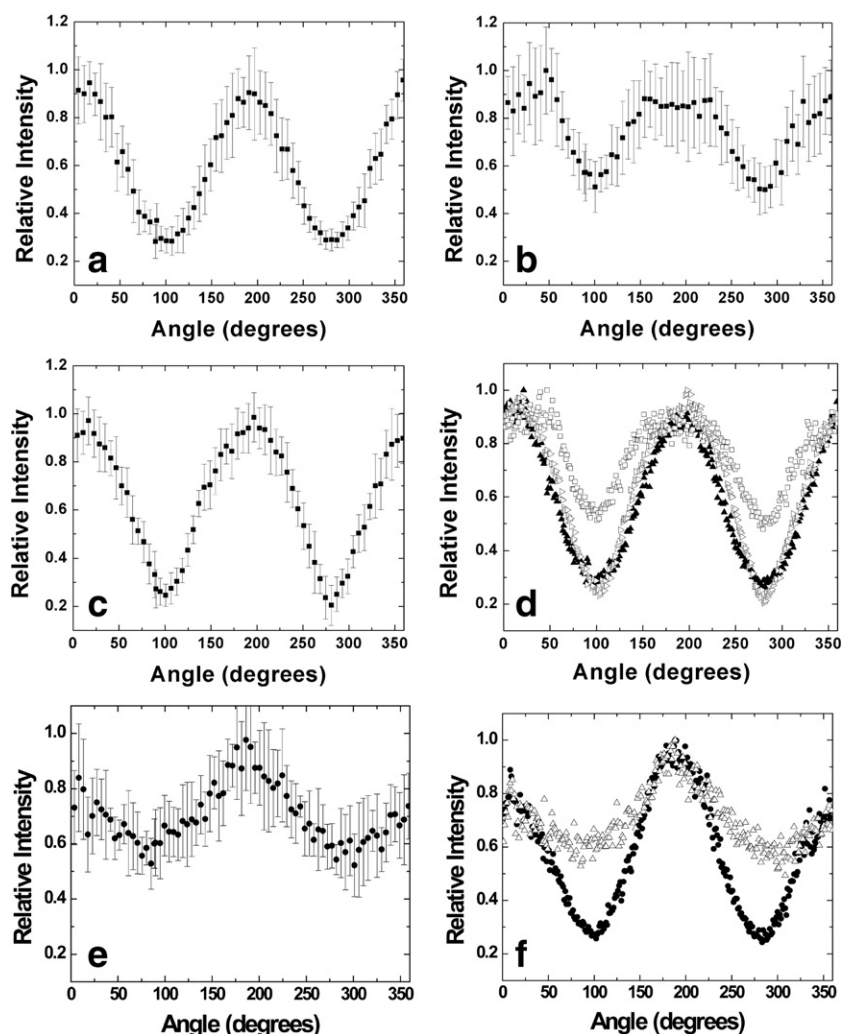


Fig. 8. Angular intensity distributions of polycyclic aromatic hydrocarbons (PAHs) in  $L_o$  phase vesicles and DOPC vesicles containing cholesterol. Intensity distributions were obtained from fluorescence images equivalent to those shown in Fig. 7, of vesicles illuminated with linearly polarized excitation light. The error bars refer to standard deviations that correspond to ten individual measurements. (a) naphthopyrene, (b) perylene, (c) terrylene, (d) a combination of the three plots for comparison. In the case of perylene, a shallower intensity profile is obtained compared to naphthopyrene and terrylene, indicating less confined orientations of perylene in  $L_o$  phase membranes. This finding parallels the partition behavior of perylene compared to naphthopyrene and terrylene. The characteristic flattening of perylene fluorescence near the maximum intensities (see panel b) could indicate two different orientational populations of this fluorophore [64]. (e) Naphthopyrene angular intensity distributions in DOPC/cholesterol=7:3 vesicles. Increased cholesterol content leads to orientational confinement of the fluorescence probe, albeit to a weaker extent compared to SPM (see the comparison in panel f of the DOPC/cholesterol=7:3 (open triangles), and SPM/cholesterol=7:3 measurements (filled circles)). Equivalent behavior is found for perylene and terrylene (data not shown).

Polycyclic aromatic hydrocarbons were found in the present study to have preference for liquid-ordered phases with some dependence on the molecular structure of the dye. The relatively high photostability of naphthopyrene, perylene, rubicene and terrylene (compared to fluorescent cholesterol analogs) makes them suitable for studying the properties of  $L_o$  phases by fluorescence methods.

All of the  $L_o$  phase-prefering PAHs consist of a planar ring system. Although the molecular details that lead to the formation of liquid-ordered phases are not yet completely understood, it is known that the cholesterol/phospholipid interaction leads to an effective stretching of the acyl chains of the phospholipids by increasing the fraction of trans-configurations in the chain [71]. Furthermore, cholesterol preferentially associates with saturated chain sphingo- and

phospholipids with high main phase transition temperature [72]. In particular, the flat  $\alpha$ -surface of cholesterol associates with long chain saturated lipids such as sphingomyelin, whereas disorder-prefering lipids such as DOPC were observed by molecular dynamics simulations not to distinguish between the  $\alpha$ -surface and the more rough  $\beta$ -surface of cholesterol [73]. The partitioning behavior of polycyclic aromatic hydrocarbons discussed above indicates that hydrophobic, disk-shaped molecules can partition preferentially into the  $L_o$  phase.

Using fluorescence microscopy with polarized excitation light, we observed that PAHs tend to align their excitation dipole moment along the membrane normal in liquid-ordered phase membranes, but not in  $L_d$  phase membranes. A recent NMR study [74] examined the orientation of pyrene, a PAH

similar in structure to the ones used in the present contribution, in lipid bilayer membranes. The normal to this disk-shaped molecule was found to align perpendicular to the membrane normal. The long axis of the molecule was found to align parallel to the membrane normal within a range of  $\pm 30^\circ$ , in a disordered phase membrane of POPC [74]. This difference with our result that PAHs are not significantly oriented in  $L_d$  phase membranes might arise from the more ordered  $L_d$  phase in the partially dehydrated multilayer films of POPC [74]. On the other hand, the conclusion that PAHs orient with their longest axis along the membrane normal [74] is in agreement with our results for  $L_o$  phase membranes. For perylene, the angular intensity profile shows an interesting flattening of the peak intensity profile compared to naphthopyrene and terrylene. This phenomenon could indicate two distinct orientational populations of the fluorophore in the membrane [67], which has been suggested previously for perylene [59].

Our study of probe partitioning has been qualitative in nature. By comparing fluorescence intensities of fluorophores in coexisting fluid phases, it should in principle be possible to obtain quantitative results, i.e. partitioning coefficients of probes in *ternary* lipid mixtures, if phase coexistence is optically resolvable. Fluorescence microscopy imaging in that sense is advantageous over spectroscopic measurements of probe partitioning, which can yield quantitative measurements of partitioning coefficients in *binary*, but not in *ternary* mixtures, unless the phase diagram tie lines are known. The probe orientation measurements described and cited above, however, indicate that a quantitative microscopy measurement of fluorescence intensities to determine partitioning coefficients has to be carefully corrected for the effect of probe orientation within the membrane.

## 5. Conclusion

We have characterized a large variety of headgroup- and chain-labeled lipid analogs, cholesterol derivatives and PAHs for their partitioning between liquid-ordered and disordered phases. The following findings can be used as a guide for selecting fluorescence probes and lipid model systems in research aimed at elucidating membrane phase behavior with fluorescence methods.

- (1) Most lipid analogs partitioned strongly out of  $L_o$  and into  $L_d$  phases.
- (2) Polycyclic aromatic hydrocarbons partitioned out of  $L_d$  and into  $L_o$  phases, or showed equal phase partitioning.
- (3) Probe partitioning was found to depend on:
  - (a) Characteristics of the fluorophore (i.e. the chain length and saturation/unsaturation of fluorescent lipid analogs and the size and molecular structure of polycyclic intercalating fluorophores);
  - (b) Nature of the host membrane lipids (DiI partitioning in the DSPC system was observed to be different from the SPM system).

Membrane fluorophore partitioning is expected to depend additionally on the mixing ratio of the host lipids, which is an effect that will be addressed in future experiments.

## Acknowledgments

We acknowledge support from the National Science Foundation (Nanobiotechnology Center, an STC Program under Agreement No. ECS-9876771), the National Institutes of Health (AI18603), and from a National Institute of Biomedical Imaging and Bioengineering-National Institutes of Health Grant 9 P41 EB001976. GWF was supported by grants from the American Chemical Society PRF 38464-AC7 and the National Science Foundation MCB-0315330.

## References

- [1] K. Simons, E. Ikonen, Functional rafts in cell membranes, *Nature* 387 (1997) 569–572.
- [2] E. Ikonen, Roles of lipid rafts in membrane transport, *Curr. Opin. Cell Biol.* 13 (2001) 470–477.
- [3] R.G. Parton, A.A. Richards, Lipid rafts and caveolae as portals for endocytosis: new insights and common mechanisms, *Traffic* 2003 (2003) 724–738.
- [4] J.B. Helms, C. Zurzolo, Lipids as targeting signals: lipid rafts and intracellular trafficking, *Traffic* 5 (2004) 247–254.
- [5] P.H.M. Lommerse, H.P. Spaank, T. Schmidt, In vivo plasma membrane organization: results of biophysical approaches, *Biochim. Biophys. Acta, Biomembr.* 1664 (2004) 119–131.
- [6] M. Edidin, The state of lipid rafts: from model membranes to cells, *Annu. Rev. Biophys. Biomol. Struct.* 32 (2003) 257–283.
- [7] W.H. Binder, V. Barragan, F.M. Menger, Domains and rafts in lipid membranes, *Angew. Chem. (Int. Ed.)* 42 (2003) 5802–5827.
- [8] R.G. Parton, J.F. Hancock, Lipid rafts and plasma membrane microorganization: insights from Ras, *Trends Cell Biol.* 14 (2004) 141–147.
- [9] L.D. Zajchowski, S.M. Robbins, Lipid rafts and little caves—Compartmentalized signalling in membrane microdomains, *Eur. J. Biochem.* 269 (2002) 737–752.
- [10] D.A. Brown, E. London, Functions of lipid rafts in biological membranes, *Annu. Rev. Cell Dev. Biol.* 14 (1998) 111–136.
- [11] S. Mayor, M. Rao, Rafts: scale-dependent, active lipid organization at the cell surface, *Traffic* 5 (2004) 231–240.
- [12] S. Munro, Lipid rafts: elusive or illusive? *Cell* 115 (2003) 377–388.
- [13] H.M. McConnell, M. Vrljic, Liquid–liquid immiscibility in membranes, *Annu. Rev. Biophys. Biomol. Struct.* 32 (2003) 469–492.
- [14] J.L. Thomas, D. Holowka, B. Baird, W.W. Webb, Large-scale coaggregation of fluorescent lipid probes with cell-surface proteins, *J. Cell Biol.* 125 (1994) 795–802.
- [15] M.M. Hao, S. Mukherjee, F.R. Maxfield, Cholesterol depletion induces large scale domain segregation in living cell membranes, *Proc. Natl. Acad. Sci. U. S. A.*, vol. 98, 2001, pp. 13072–13077.
- [16] A. Gidwani, D. Holowka, B. Baird, Fluorescence anisotropy measurements of lipid order in plasma membranes and lipid rafts from RBL-2H3 mast cells, *Biochemistry* 40 (2001) 12422–12429.
- [17] K. Gaus, E. Gratton, E.P.W. Kable, A.S. Jones, I. Gelissen, L. Kritharides, W. Jessup, Visualizing lipid structure and raft domains in living cells with two-photon microscopy, *Proc. Natl. Acad. Sci. U. S. A.*, vol. 100, 2003, pp. 15554–15559.
- [18] R. Varma, S. Mayor, GPI-anchored proteins are organized in submicron domains at the cell surface, *Nature* 394 (1998) 798–801.
- [19] A. Kusumi, H. Ike, C. Nakada, K. Murase, T. Fujiwara, Single-molecule tracking of membrane molecules: plasma membrane compartmentalization and dynamic assembly of raft-philic signaling molecules, *Semin. Immunol.* 17 (2005) 3–21.



- [20] W.L.C. Vaz, E. Melo, Fluorescence spectroscopic studies on phase heterogeneity in lipid bilayer membranes, *J. Fluoresc.* 11 (2001) 255–271.
- [21] N.C. Santos, M. Prieto, M.A.R.B. Castanho, Quantifying molecular partition into model systems of biomembranes: an emphasis on optical spectroscopic methods, *Biochim. Biophys. Acta, Biomembr.* 1612 (2003) 123–135.
- [22] L. Davenport, Fluorescence probes for studying membrane heterogeneity, *Methods Enzymol.* 278 (1997) 487–512.
- [23] A.V. Samsonov, I. Mihalyov, F.S. Cohen, Characterization of cholesterol-sphingomyelin domains and their dynamics in bilayer membranes, *Biophys. J.* 81 (2001) 1486–1500.
- [24] C. Dietrich, L.A. Bagatolli, Z.N. Volovyk, N.L. Thompson, M. Levi, K. Jacobson, E. Gratton, Lipid rafts reconstituted in model membranes, *Biophys. J.* 80 (2001) 1417–1428.
- [25] S.L. Veatch, S.L. Keller, Organization in lipid membranes containing cholesterol, *Phys. Rev. Lett.* 89 (2002) 268101–1–268101-4.
- [26] S.L. Veatch, S.L. Keller, Separation of liquid phases in giant vesicles of ternary mixtures of phospholipids and cholesterol, *Biophys. J.* 85 (2003) 3074–3083.
- [27] N. Kahya, D. Scherfeld, K. Bacia, B. Poolman, P. Schwille, Probing lipid mobility of raft-exhibiting model membranes by fluorescence correlation spectroscopy, *J. Biol. Chem.* 278 (2003) 28109–28115.
- [28] T. Baumgart, S.T. Hess, W.W. Webb, Imaging coexisting fluid domains in biomembrane models coupling curvature and line tension, *Nature* 425 (2003) 821–824.
- [29] L.A. Bagatolli, E. Gratton, Two-photon fluorescence microscopy observation of shape changes at the phase transition in phospholipid giant unilamellar vesicles, *Biophys. J.* 77 (1999) 2090–2101.
- [30] J. Korlach, P. Schwille, W.W. Webb, G.W. Feigenson, Characterization of Lipid Bilayer Phases by Confocal Microscopy and Fluorescence Correlation Spectroscopy, *Proc. Natl. Acad. Sci. U. S. A.*, vol. 96, 1999, pp. 8461–8466.
- [31] G.W. Feigenson, J.T. Buboltz, Ternary phase diagram of dipalmitoyl-PC/dilauroyl-PC/cholesterol: nanoscopic domain formation driven by cholesterol, *Biophys. J.* 80 (2001) 2775–2788.
- [32] S.L. Veatch, S.L. Keller, Miscibility phase diagrams of giant vesicles containing sphingomyelin, *Phys. Rev. Lett.* 94 (2005).
- [33] R.D. Klausner, D.E. Wolf, Selectivity of fluorescent lipid analogues for lipid domains, *Biochemistry* 19 (1980) 6199–6203.
- [34] N.-n. Huang, K. Florin-Casteel, G.W. Feigenson, C.H. Spink, Effects of fluorophore Linkage Position of n-(9-anthroxyl) fatty acids on probe distribution between coexisting gel and fluid phospholipid phases, *Biochim. Biophys. Acta* 939 (1988) 124–130.
- [35] C.H. Spink, M.C. Yeager, G.W. Feigenson, Partitioning behavior of indocarbocyanine probes between coexisting gel and fluid phase model membranes, *Biochim. Biophys. Acta* 1023 (1990) 25–33.
- [36] A. Beck, D. Heissler, G. Duportail, Influence of the length of the spacer on the partitioning properties of amphiphilic fluorescent membrane probes, *Chem. Phys. Lipids* 66 (1993) 135–142.
- [37] L.M.S. Loura, A. Fedorov, M. Prieto, Partition of membrane probes in a gel/fluid two-component lipid system: a fluorescence resonance energy transfer study, *Biochim. Biophys. Acta* 1467 (2000) 101–112.
- [38] R.M.R.S. Mesquita, E. Melo, T.E. Thompson, W.L.C. Vaz, Partitioning of amphiphiles between coexisting ordered and disordered phases in two-phase lipid bilayer membranes, *Biophys. J.* 78 (2000) 3019–3025.
- [39] A. Pokorny, P.F.F. Almeida, W.L.C. Vaz, Association of a fluorescent amphiphile with lipid bilayer vesicles in regions of solid–liquid-disordered phase coexistence, *Biophys. J.* 80 (2001) 1384–1394.
- [40] T.Y. Wang, J.R. Silvius, Different sphingolipids show differential partitioning into sphingolipid/cholesterol-rich domains in lipid bilayers, *Biophys. J.* 79 (2000) 1478–1489.
- [41] T.Y. Wang, R. Leventis, J.R. Silvius, Fluorescence evaluation of molecular partitioning into lipid ‘rafts’ (liquid-ordered domains) in lipid model membranes, *Mol. Biol. Cell* 11 (2000) 4a–5a.
- [42] T.Y. Wang, R. Leventis, J.R. Silvius, Partitioning of lipidated peptide sequences into liquid-ordered lipid domains in model and biological membranes, *Biochemistry* 40 (2001) 13031–13040.
- [43] T.-Y. Wang, J.R. Silvius, Sphingolipid-partitioning into ordered domains in cholesterol-free and cholesterol containing lipid bilayers, *Biophys. J.* 84 (2003) 367–378.
- [44] M. Koivusalo, J. Alvesalo, J.A. Virtanen, P. Somerharju, Partitioning of pyrene-labeled phospho- and sphingolipids between ordered and disordered bilayer domains, *Biophys. J.* 86 (2004) 923–935.
- [45] H.J. Gruber, H. Schindler, External surface and lamellarity of lipid vesicles—A practice-oriented set of assay-methods, *Biochim. Biophys. Acta, Biomembr.* 1189 (1994) 212–224.
- [46] R.T. Fischer, F.A. Stephenson, A. Shafiee, F. Schroeder, Delta-5,7,9(11)-cholestatien-3beta-ol—A fluorescent cholesterol analog, *Chem. Phys. Lipids* 36 (1984) 1–14.
- [47] K. Akashi, H. Miyata, H. Itoh, K. Kinoshita, Preparation of giant liposomes in physiological conditions and their characterization under an optical microscope, *Biophys. J.* 71 (1996) 3242–3250.
- [48] L. Mathivet, S. Cribier, P.F. Devaux, Shape change and physical properties of giant phospholipid vesicles prepared in the presence of an AC electric field, *Biophys. J.* 70 (1996) 1112–1121.
- [49] A.G. Ayuyan, F.S. Cohen, Lipid peroxides promote large rafts: effects of excitation of probes in fluorescence microscopy and electrochemical reactions during vesicle formation, *Biophys. J.* 91 (2006) 2172–2183.
- [50] O. Maier, V. Oberle, D. Hoekstra, Fluorescent lipid probes: some properties and applications (a review), *Chem. Phys. Lipids* 116 (2002) 3–18.
- [51] R. Gagescu, N. Demaurex, R.G. Parton, W. Hunziker, L.A. Huber, J. Gruenberg, The recycling endosome of Madin–Darby canine kidney cells is a mildly acidic compartment rich in raft components, *Mol. Biol. Cell* 11 (2000) 2775–2791.
- [52] V. Puri, R. Watanabe, R.D. Singh, M. Dominguez, J.C. Brown, C.L. Wheatley, D.L. Marks, R.E. Pagano, Clathrin-dependent and -independent internalization of plasma membrane sphingolipids initiates two Golgi targeting pathways, *J. Cell Biol.* 154 (2001) 535–547.
- [53] R.J. Schroeder, S.N. Ahmed, Y.Z. Zhu, E. London, D.A. Brown, Cholesterol and sphingolipid enhance the Triton X-100 insolubility of glycosylphosphatidylinositol-anchored proteins by promoting the formation of detergent-insoluble ordered membrane domains, *J. Biol. Chem.* 273 (1998) 1150–1157.
- [54] D. Scherfeld, N. Kahya, P. Schwille, Lipid dynamics and domain formation in model membranes composed of ternary mixtures of unsaturated and saturated phosphatidylcholines and cholesterol, *Biophys. J.* 85 (2003) 3758–3768.
- [55] S.L. Veatch, I.V. Polozov, K. Gawrisch, K.S.L. Keller, Liquid domains in vesicles investigated by NMR and fluorescence microscopy, *Biophys. J.* 86 (2004) 2910–2922.
- [56] H.A. Scheidt, P. Mueller, A. Herrmann, D. Huster, The potential of fluorescent and spin-labeled steroid analogs to mimic natural cholesterol, *J. Biol. Chem.* 278 (2003) 45563–45569.
- [57] J.R. Lakowicz, J.R. Knutson, Hindered depolarizing rotations of perylene in lipid bilayers—Detection by lifetime-resolved fluorescence anisotropy measurements, *Biochemistry* 19 (1980) 905–911.
- [58] P.L.-G. Chong, B.W. van der Meer, T.E. Thompson, The effects of pressure and cholesterol on rotational motions of perylene in lipid bilayers, *Biochim. Biophys. Acta* 813 (1984) 253–265.
- [59] M.A.M.J. Zandvoort, H.C. Gerritsen, g. vanGinkel, Y.K. Levine, R. Tarroni, C. Zannoni, Distribution of hydrophobic probe molecules in lipid bilayers. 2. Time-resolved fluorescence anisotropy study of perylene in vesicles, *J. Phys. Chem.*, B 101 (1997) 4149–4154.
- [60] A. Rademacher, S. Maerkele, H. Langhals, Loesliche Perylen-Fluoreszenzfarbstoffe mit hoher Photostabilitaet, *Chem. Ber.* 115 (1982) 2927–2934.
- [61] J.R. Knutson, L. Davenport, L. Brand, Anisotropy decay associated fluorescence-spectra and analysis of rotational heterogeneity .1. Theory and applications, *Biochemistry* 25 (1986) 1805–1810.
- [62] B.R. Lentz, Use of fluorescent-probes to monitor molecular order and motions within liposome bilayers, *Chem. Phys. Lipids* 64 (1993) 99–116.
- [63] B.R. Lentz, D.A. Barrow, M. Hoechli, Cholesterol–phosphatidylcholine interactions in multilamellar vesicles, *Biochemistry* 19 (1980) 1943–1954.
- [64] D. Axelrod, Carbocyanine dye orientation in red-cell membrane studied by microscopic fluorescence polarization, *Biophys. J.* 26 (1979) 557–573.
- [65] K. Florine-Casteel, Phospholipid order in gel-phase and fluid-phase cell-

- size liposomes measured by digitized video fluorescence polarization microscopy, *Biophys. J.* 57 (1990) 1199–1215.
- [66] L.A. Bagatolli, E. Gratton, Two photon fluorescence microscopy of coexisting lipid domains in giant unilamellar vesicles of binary phospholipid mixtures, *Biophys. J.* 78 (2000) 290–305.
- [67] K. Florine-Casteel, *Video Imaging of Lipid Order*, Elsevier, 1999.
- [68] D.E. Warschawski, P.F. Devaux, Order parameters of unsaturated phospholipids in membranes and the effect of cholesterol: a H-1-C-13 solid-state NMR study at natural abundance, *Eur. Biophys. J. Biophys. Lett.* 34 (2005) 987–996.
- [69] W. Guo, V. Kurze, T. Huber, N.H. Afdhal, K. Beyer, J.A. Hamilton, A solid-state NMR study of phospholipid–cholesterol interactions: sphingomyelin–cholesterol binary systems, *Biophys. J.* 83 (2002) 1465–1478.
- [70] H. Ohvo-Rekila, B. Ramstedt, P. Leppimäki, J.P. Slotte, Cholesterol interactions with phospholipids in membranes, *Prog. Lipid Res.* 41 (2002) 66–97.
- [71] M.B. Sankaram, T.E. Thompson, Modulation of phospholipid acyl chain order by cholesterol. A solid-state <sup>2</sup>H nuclear magnetic resonance study, *Biochemistry* 29 (1990) 10676–10684.
- [72] J.R. Silvius, Role of cholesterol in lipid raft formation: lessons from lipid model systems, *Biochim. Biophys. Acta* 1610 (2003) 174–183.
- [73] S.A. Pandit, E. Jakobsson, H.L. Scott, Simulation of the early stages of nano-domain formation in mixed bilayers of sphingomyelin, cholesterol, and dioleoylphosphatidylcholine, *Biophys. J.* 87 (2004) 3312–3322.
- [74] B. Hoff, E. Strandberg, A.S. Ulrich, D.P. Tieleman, C. Posten, H-2-NMR study and molecular dynamics simulation of the location, alignment, and mobility of pyrene in POPC bilayers, *Biophys. J.* 88 (2005) 1818–1827.